Monthly Notices
of the
ROYAL ASTRONOMICAL SOCIETY

Mon. Not. R. Astron. Soc. (2011) doi:10.1111/j.1365-2966.2011.20154.x

A hierarchy of voids: more ado about nothing

Aseem Paranjape,[1⋆] Tsz Yan Lam[2⋆] and Ravi K. Sheth[1,3]

[1]*The Abdus Salam ICTP, Strada Costiera 11, 34151 Trieste, Italy*
[2]*IPMU, University of Tokyo, Kashiwa, Chiba 277-8583, Japan*
[3]*Center for Particle Cosmology, University of Pennsylvania, 209 S. 33rd St., Philadelphia, PA 19104, USA*

Accepted 2011 November 7. Received 2011 November 3; in original form 2011 June 22

ABSTRACT

We extend earlier work on the problem of estimating the void-volume function – the abundance and evolution of large voids which grow gravitationally in an expanding universe – in two ways. The first removes an ambiguity about how the void-in-cloud process, which erases small voids, should be incorporated into the excursion set approach. The main technical change here is to think of voids within a fully Eulerian, rather than purely Lagrangian, framework. The second accounts for correlations between different spatial scales in the initial conditions. We provide numerical and analytical arguments showing how and why both changes modify the predicted abundances substantially. In particular, we show that the predicted importance of the void-in-cloud process depends strongly on whether or not one accounts for correlations between scales. With our new formulation, the void-in-cloud process dramatically reduces the predicted abundances of voids if such correlations are ignored, but only matters for the smallest voids in the more realistic case in which the spatial correlations are included.

Key words: large-scale structure of Universe.

1 INTRODUCTION

The abundance of clusters and its evolution is a useful probe of the primordial fluctuation field, the subsequent expansion history of the Universe and the nature of gravity. This is, in part, because there is an analytic framework for understanding how cluster formation and evolution depends on the background cosmological model (Gunn & Gott 1972; Press & Schechter 1974; Peacock & Heavens 1990; Bond et al. 1991; Sheth, Mo & Tormen 2001; Martino, Stabenau & Sheth 2009).

If the clusters were identified in a galaxy survey, then it is possible to identify underdense regions – voids – in the same data set (e.g. Kauffmann & Fairall 1991; Hoyle & Vogeley 2004; Hoyle et al. 2005; Patiri et al. 2006b; Pan et al. 2011). As for the clusters, there exists an analytic framework for understanding void formation (Blumenthal et al. 1992; Dubinski et al. 1993; van de Weygaert & van Kampen 1993; Sheth & van de Weygaert 2004; Furlanetto & Piran 2006; Patiri, Betancort-Rijo & Prada 2006a), so the comoving number density of voids of radius R, and its evolution, provides complementary information about cosmology (Kamionkowski, Verde & Jimenez 2009; Lam, Sheth & Desjacques 2009; D'Amico et al. 2011) and gravity (Martino & Sheth 2009). Void shapes are interesting too (Park & Lee 2007; Biswas, Alizadeh & Wandelt 2010; Lavaux & Wandelt 2010), but they are not the primary interest of this paper.

Following Press & Schechter (1974), studies of cluster and void evolution relate the formation of an object to its initial overdensity. A cluster today is a region that is about 200 times the background density, and it formed from the collapse of a sufficiently overdense region in the initial conditions. However, the overdensity associated with a given position in space depends on scale (in homogeneous cosmologies, the likely range of overdensities is smaller on large scales). So, to estimate cluster abundances, the problem is to find those regions in the initial conditions which are sufficiently overdense on a given smoothing scale, but not on a larger scale. This is because, if the larger region is sufficiently overdense, then, as it pulls itself together against the expansion of the background universe and collapses, it will also squeeze the regions within it to smaller and smaller sizes. The framework for not double-counting the smaller overdense clouds that are embedded in larger overdense clouds is known as the excursion set approach (Epstein 1983; Bond et al. 1991; Lacey & Cole 1993; Sheth 1998).

For voids – regions that today are about 20 per cent the background density – the problem is slightly more complicated, since one must account not just for the analogous void-in-void problem, but also for the fact that underdensities which are surrounded by sufficiently overdense shells will be crushed as the overdensity collapses around them. This void-in-cloud problem was identified by Sheth & van de Weygaert (2004), who also showed how one might account for both the void-in-void and the void-in-cloud problems in the language of the excursion set approach.

However, their formulation suffers from an important drawback – they treat the identification of the overdensity associated with a cloud as a single scale independent number. As they noted, it is

⋆E-mail: aparanja@ictp.it (AP); tszyan.lam@ipmu.jp (TYL)

easy to see that this is, at best, a crude approximation. Suppose that this number is that associated with the formation of a cluster. Then, their approach corresponds to eliminating from the list of all possible voids all those that are surrounded by an initially larger region which is destined to have collapsed and formed a cluster by the time the void they surround would have formed (were it not surrounded by this overdensity). This leads to the question of what to do with sufficiently underdense regions which were surrounded by regions which will not have collapsed completely by the time the void inside them forms, but that will nevertheless have squeezed the enclosed void, thus altering its size, and possibly even preventing its formation.

To illustrate the magnitude of this effect, Sheth & van de Weygaert showed how the predicted void abundances change if one uses the overdensity associated with 'cloud' turnaround instead of collapse (the two differ by approximately a factor of 1.6 in initial overdensity). While the difference for big voids is small – big underdense regions are unlikely to be surrounded by even larger overdensities – the effect on smaller voids is dramatic. Although it is the largest voids which are most easily measured, and so most likely to place the most interesting constraints on cosmological models, the uncertainty from not knowing precisely where the void-in-cloud problem becomes relevant is problematic. (One way to view this problem is to note that large voids are exponentially rare, so to constrain cosmology requires large survey volumes. By having an accurate model of smaller voids, one potentially allows smaller surveys to place interesting constraints.)

The main goal of the current paper is to present a formulation of the problem which resolves this drawback of the initial formulation. The key is to phrase the criterion for being a void in terms of the late-time field – a void is the largest region in the late-time field which is sufficiently underdense – and to then determine what this requires of the initial field. This means one must be able to relate what are often called Eulerian volumes in the late-time field, and Lagrangian ones in the initial field. Fortunately, this can be done within the excursion set approach (Sheth 1998; Lam & Sheth 2008).

However, there turn out to be a number of subtleties along the way, which are related to one of the technical assumptions associated with the excursion set approach. Strictly speaking, the overdensity associated with a given position and scale is correlated with the overdensity on all other smoothing scales as well. Therefore, if one plots this overdensity as a function of smoothing scale, then this looks like a random walk with correlated steps. Following Bond et al. (1991), most excursion set analyses, and the Sheth & van de Weygaert model for voids in particular, make the approximation that the steps are uncorrelated, and they then assume that the resulting prediction will be a useful approximation to that which one would have obtained if one had solved the (more physically relevant) correlated steps problem. Accounting for such correlations makes relatively minor changes to the cloud-in-cloud (or void-in-void) predictions (Peacock & Heavens 1990; Maggiore & Riotto 2010; Paranjape et al. 2011). In what follows, we will show that the difference between the correlated and uncorrelated solutions is much larger for the void-in-cloud problem.

In Section 2 we show how to cleanly resolve the void-in-cloud issue in the excursion set approach. In Section 3, we use a numerical Monte Carlo method to show that the uncorrelated steps formulation is quite sensitive to this change – our solution to the void-in-cloud problem predicts far fewer large voids than do Sheth & van de Weygaert. On the other hand, the correlated steps formulation is almost completely unaffected by the void-in-cloud problem in the first place, and so is not sensitive to the change in our prescription. In other words, the void-in-cloud problem is a case in which the difference between correlated and uncorrelated steps matters greatly. A final section discusses some implications.

2 A BETTER MODEL OF THE VOID-IN-CLOUD PROBLEM

In this section, we show how a more careful statement of the void-in-cloud process leads to a slightly modified formulation of the problem in the excursion set approach. In essence, this resolution of the problem combines the analysis in Sheth & van de Weygaert (2004) with that in Sheth (1998).

2.1 Lagrangian versus Eulerian treatments

In what follows, we will denote the Eulerian radius and volume of the void by R and V, respectively (so that $V = 4\pi R^3/3$), and refer to Lagrangian length-scales simply through the associated mass $m = \bar{\rho}(4\pi R_{\rm L}^3/3)$, where $\bar{\rho}$ is the comoving background density and $R_{\rm L}$ is the Lagrangian radius which evolved into the Eulerian radius R. We will also use $s(m)$ to denote the variance of the linearly extrapolated density contrast when filtered on a Lagrangian scale corresponding to mass m: $s(m) = (2\pi^2)^{-1}\int_0^\infty {\rm d}k\, k^2 P(k) W^2(kR_{\rm L})$, where $W(kR_{\rm L})$ is the filter and $P(k)$ the linearly evolved matter power spectrum.

The condition for being identified as a void of Eulerian size R at some time t is that the region of size R must be (a) less dense than some critical threshold (typically about 20 per cent of the background density); (b) denser than this critical threshold value on all larger Eulerian scales. Sheth & van de Weygaert replaced these Eulerian conditions with Lagrangian ones. The Lagrangian region of mass scale M must be ($a_{\rm L}$) less dense than some critical density initially (typically, linear theory overdensity of -2.71), ($b_{\rm L}$) denser than this on all larger mass scales and ($c_{\rm L}$) not dense enough on these larger Lagrangian scales for this to have influenced the evolution of the initial void-candidate region sufficiently that it did not form a void at late times.

Sheth & van de Weygaert argued that these requirements correspond to two different barriers in the excursion set approach. In the plane of (linearly extrapolated) initial overdensity versus scale, the first two requirements correspond to the first crossing of a barrier of constant height $\delta_{\rm v}$. (When extrapolated to the present time using linear theory, $\delta_{\rm v} = -2.71$, approximately independent of the background cosmology, and this fixes the void mass as $M \approx 0.2\bar{\rho}V$, see below.) At issue is how best to implement the last constraint ($c_{\rm L}$), i.e. how to remove from the list of potential voids identified in the initial conditions, those which would not also be identified as voids at later times (i.e. in the Eulerian field).

Sheth & van de Weygaert assumed that this could be done simply by introducing a second barrier, B: of the set of walks which first cross $\delta_{\rm v}$ at the Lagrangian scale corresponding to the void mass M, one must remove those which crossed B before (i.e. at some mass $m > M$) they crossed $\delta_{\rm v}$. They assumed that $B = \delta_{\rm c} =$ constant (and hence parallel to $\delta_{\rm v}$), where $\delta_{\rm c}$ is the initial overdensity required for collapse at some time t, extrapolated using linear theory to time t (if $\delta_{\rm v} = -2.71$ then $\delta_{\rm c} = 1.686$).[1] This would

[1] Strictly speaking, the exact values of $\delta_{\rm c}$ and $\delta_{\rm v}$ depend weakly on the cosmological parameters; the values quoted above correspond to the Einstein–deSitter case. Our focus, however, is on conceptual issues rather than numerical accuracy, and our discussion does not depend on the exact numerical values of these parameters.

correspond to excluding regions which surround the void candidate region and have collapsed by time t, thus completely squeezing out the void.

In our new approach, which allows us to account for regions which have only partially squeezed the void (and were not excluded by Sheth & van de Weygaert), it turns out to be more straightforward to not mix-and-match conditions in Eulerian and Lagrangian space. Rather, we will work entirely with the conditions (a) and (b) stated in Eulerian space, and we will draw on the analysis in Sheth (1998) to implement these Eulerian conditions in the (essentially Lagrangian) plane of initial overdensity versus scale.

2.2 The Eulerian treatment

To begin, one notes that the spherical evolution model relates the Eulerian overdensity $\Delta_{\rm NL} \equiv m/(\bar\rho V)$, where m is the mass in a region that has volume V at time t, to the linearly extrapolated density contrast $\delta(t)$ by

$$\Delta_{\rm NL}(t) = \frac{m}{\bar\rho V} \approx \left(1 - \frac{\delta(t)}{\delta_{\rm c}}\right)^{-\delta_{\rm c}} \qquad (1)$$

(Bernardeau 1994). If $V = 4\pi R^3/3$ is specified, then this relation defines a curve $B_V(m)$ which gives the value of the linearly extrapolated density contrast in a Lagrangian region containing mass m which evolves into the Eulerian volume V at time t:

$$B_V(m) = \delta_{\rm c}\left[1 - \left(\frac{m}{\bar\rho V}\right)^{-1/\delta_{\rm c}}\right]. \qquad (2)$$

Notice that $B_V(m) \to \delta_{\rm c}$ at $m \gg \bar\rho V$, but that it decreases monotonically as m decreases, crossing 0 at $m = \bar\rho V$, and eventually crossing $\delta_{\rm v}$ at m sufficiently smaller than $\bar\rho V$. In addition, note that setting $\delta(t) = -2.71$ and $\delta_{\rm c} = 1.686$ makes $\Delta_{\rm NL} \approx 0.2$, implying a void mass of $M \approx 0.2\bar\rho V$ for a void of Eulerian volume V. And finally, thinking of V as a parameter, note that decreasing V defines a sequence of nested curves whose limit, as $V \to 0$, is the constant barrier $\delta_{\rm c}$: $B_{V\to 0}(m) \to \delta_{\rm c}$.

The dotted lines in Fig. 1 show such a nested sequence. Also shown are two candidate random walks (blue and red solid lines) which first cross $\delta_{\rm v}$ at the same Lagrangian mass scale $S = s(M)$, so that $B_V(M) = \delta_{\rm v}$. Since neither of these walks exceeded $\delta_{\rm c}$ prior to first crossing $\delta_{\rm v}$, Sheth & van de Weygaert would have assigned both walks the same Lagrangian mass and Eulerian volume.

For us, the two walks are rather different void candidates. This is because the mass inside Eulerian V at time t is given by the value of $s(m)$ at which the associated barrier $B_V(m)$ is first crossed (Sheth 1998). For the (blue) walk which decreases monotonically, the monotonicity in Lagrangian δ translates directly into a monotonicity in $\Delta_{\rm NL}$, so that conditions (a), (b) as well as ($a_{\rm L}$), ($b_{\rm L}$) and ($c_{\rm L}$) are all met. For the void associated with this walk, we would assign the same mass and volume as would Sheth & van de Weygaert. In particular, the Eulerian volume would lie between V_3 and V_2.

However, for the other (red) walk, the non-monotonicity of δ means that $\Delta_{\rm NL}$ is not monotonic either. More importantly, although the predicted mass decreases monotonically with Eulerian V, it need not do so smoothly. Rather, on scales V where B_V is tangent to the walk, the predicted mass must jump downwards as $V \to V - \Delta V$ (i.e. as the barrier is made shallower), because the value of s on which $B_{V-\Delta V}$ is first crossed can be substantially larger than that on which B_V was first crossed. (In the figure, this happens at about V_2.) This means that, for the entire portion of the walk between these two first crossing values (essentially, the value of s at which a barrier

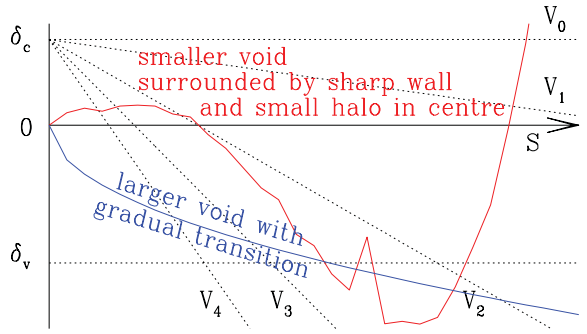

Figure 1. Excursion set model of voids. Dotted lines show the 'barriers' associated with Eulerian volumes $V_4 > V_3 > V_2 > V_1 > V_0$: barriers for larger volumes fall more steeply. The horizontal line at $\delta_{\rm v} = -2.71$ shows the critical linearly extrapolated initial density for voids. Solid lines show two examples of random walks; both first-cross $\delta_{\rm v}$ on the same mass scale S. Since neither walk crossed $\delta_{\rm c}$ prior to crossing $\delta_{\rm v}$, Sheth & van de Weygaert would have assigned the same void mass and Eulerian volume to both walks. However, in our prescription, the (blue) one which falls monotonically with S is associated with a larger Eulerian volume (between V_3 and V_2), because its evolution is not modified by the void-in-cloud process: we would have assigned the same mass and volume to it as they did. The other (red) walk represents an overdensity on the Eulerian scale V_2 (because V_2 is first crossed at $\delta > 0$), but a void on the Eulerian scale just smaller than this (because the first crossing of the next shallower barrier will be at $\delta < \delta_{\rm v}$). The evolution of this void has been modified by the collapse of the overdensity surrounding it. We would assign a larger mass to the 'wall' which surrounds the void, and a smaller mass and volume to the void itself, compared to Sheth & van de Weygaert. Moreover, note that, for this walk, the first crossing of $\delta_{\rm v}$ is actually not so significant.

B_V is tangent to the walk, and the next larger value of s at which it pierces the walk), translating the Lagrangian δ to an Eulerian $\Delta_{\rm NL}$ using equation (1) will *not* yield the correct answer. This, in essence, is why an approach based purely on Lagrangian quantities will not work: one *must* use Eulerian quantities. This sharp transition in mass (and hence Eulerian density) at nearly constant Eulerian volume has a clean physical interpretation in terms of a dense 'wall' surrounding the underdense void. In the current instance, we would assign the void a Eulerian volume that is essentially V_2, with mass interior to the void given by the value of s at which B_{V_2} intersects the walk. And we would interpret the value of s at which B_{V_2} was tangent to the walk as the mass at the void wall.

For this particular walk, the two masses can be quite different indicating that the Eulerian void should be rather well delineated by the surrounding Eulerian overdensity. This is precisely the type of void that is easiest to identify observationally – so it is worth noting that it is for just such voids that our algorithm can differ substantially from that of Sheth & van de Weygaert. The voids on which we would agree are those associated with walks that are similar to the monotonically decreasing walk in Fig. 1. Since these correspond to voids for which there is no obvious defining 'wall', they are hardest to define observationally.

To highlight how different our algorithm is, it is worth contrasting the role played by $\delta_{\rm v}$ in the two approaches. In the old one, first crossings of $\delta_{\rm v}$ are fundamental, because they give the superset of Lagrangian void candidates from which one discards those which first crossed $\delta_{\rm c}$, on the basis that they represent voids that would have been crushed out of existence by Eulerian evolution. One might have thought that, because it accounts for the squeezing rather than complete crushing of these regions due to Eulerian

evolution, our modification mainly serves to reduce the predicted volumes of the ones which remain. While this is correct, there is a subtlety.

As Fig. 1 shows, if the first crossing of δ_v happens to lie in a region where the $\delta - \Delta_{NL}$ mapping of equation (1) does not apply, then it is simply not as important as subsequent crossings of δ_v. For example, suppose the spike in the walk were higher, so that it crossed above B_{V_2} for a while, before dropping down to and zigzagging around δ_v a few times. Then the Eulerian region just within V_2 would not be a void (because the walk crossed B_{V_2} above δ_v), but one of the subsequent zigzags around δ_v might actually be the one which first crosses a Eulerian B_V, and so represents a squeezed Eulerian void. This one would certainly have a smaller volume than that given to the initial first crossing candidate by Sheth–van de Weygaert, but clearly, although δ_v plays an important role, the first crossing of δ_v is not necessarily the most relevant one. The fact that the first crossing of δ_v is no longer so important is one reason why we have been unable to derive an analytic expression for the distribution of void volumes associated with our new formulation of the void-in-cloud problem. We discuss this further in Appendix A. It is, of course, straightforward to implement our algorithm numerically, and we describe this in the next section.

But before we do so, we note that our new approach helps alleviate one unphysical feature of the old model. Namely, in the Sheth–van de Weygaert approach, the volume fraction covered by voids is $5\delta_c/(\delta_c + |\delta_v|)$. Since $\delta_c \approx 1.686$ and $|\delta_v| \approx 2.71$, this 'fraction' is nearly 2. It is easy to see that this fraction must be smaller in our new approach, because we would assign a smaller Eulerian volume to each of the Sheth–van de Weygaert void candidates (in some cases, this volume is vanishingly small). We show below that the associated void covering fraction is 1.17, i.e. although it is still greater than unity, the problem is now 20 per cent rather than 100 per cent.

2.3 Correlated versus uncorrelated steps

We expect our model predictions to depend on whether or not the steps in the random walk are correlated. For walks with uncorrelated steps, the solution to the two-barrier Lagrangian void-in-cloud problem δ_v–δ_c is quite different from that for the single δ_v barrier void-in-void problem; it has far fewer small voids (Sheth & van de Weygaert 2004). We expect our purely Eulerian void-in-cloud algorithm to produce even smaller voids, so that all three estimates of the void distribution should differ substantially from one another.

However, we expect these three estimates of void abundances to be rather similar for walks with correlated steps. This is because correlated steps generally result in smoother walks. Indeed, Paranjape et al. (2011) have recently shown that the limiting case of completely correlated steps, in which the walk height on one scale S completely specifies its height on all other s via $\delta(S)/\sqrt{S} = \delta(s)/\sqrt{s}$, actually provides a useful way of thinking about the single barrier problem. In this limit, walks do not zigzag at all, which, in the present context means that the void-in-cloud problem *never* arises, so the solution to the single barrier case δ_v would be the same as that for the purely Lagrangian (Sheth–van de Weygaert) formulation of the void-in-cloud problem (since no walks will have crossed δ_c prior to crossing δ_v). Since our algorithm is basically the same as Sheth–van de Weygaert for smooth monotonically decreasing walks, the prediction associated with our Eulerian void-in-cloud formulation would also reduce to the first crossing distribution for the single barrier of height δ_v. We expect to see differences between these three cases as we move away from the completely correlated limit. However, since Paranjape et al. have already shown that this limit is essentially exact for the most massive objects, we only expect to see differences for low-mass voids. Walks with uncorrelated steps are far from this limit, so in this case we expect to see differences appear at larger masses. The next section shows that the predicted importance of the void-in-cloud effect does indeed depend on whether or not one accounts for correlations between steps.

3 NUMERICAL (MONTE CARLO) SOLUTION

Before we show the numerical Monte Carlo solution of our algorithm, note that although the description above is general, it simplifies considerably for power spectra with $P(k) \propto k^n$ with $n = -1.2$. In this case, $s \propto m^{-(n+3)/3} \propto m^{-3/5} \sim m^{-1/\delta_c}$, so the barrier shape becomes linear in s, and this simplifies the numerical analysis considerably. For this reason, we have chosen to present results for this case first. We show results for a cold dark matter (CDM) power spectrum at the end of this section.

Our Monte Carlo algorithm works as follows. For a walk with uncorrelated steps (corresponding to a filter that is sharp in k-space), we accumulate independent Gaussian random numbers g_i with a fixed variance Δs, $\delta_j^{(\rm uncorr)} = \sum_{i=1}^{j} g_i$, and record the step at which the barrier δ_v was first crossed as well as the step at which δ_c was first crossed. The distribution of s at which δ_v was first crossed represents the solution to the void-in-void problem; that of the subset of walks for which δ_v was first crossed prior to ever crossing δ_c represents the Sheth–van de Weygaert algorithm. The black filled and open symbols in Fig. 2 show these two distributions, respectively: the solid black curves going through them show the associated analytic expressions (from Bond et al. 1991; Sheth & van de Weygaert 2004; equation A4). The agreement indicates that the numerical algorithm works.

The cyan histogram shows the result of implementing our algorithm as follows. For a walk that crossed δ_v at least once, we choose all steps prior to the first crossing. At each step j we have a pair (δ_j, s_j) which together define a Eulerian volume V_j. (In more detail, the value s_j gives a mass m_j, and insertion of δ_j in equation 1 yields $m_j/\bar{\rho}V_j$.) We call the smallest value of V_j associated with the walk so far $V_{\rm min}$. If $V_{\rm min} = 0$, we stop – this would only have happened if the walk exceeded δ_c. Since this would mean the void candidate has been crushed out of existence, we eliminate the walk from the list of void walks. If $V_{\rm min} > 0$, then asking that it be a void sets a mass $M_{\rm min} \approx 0.2\bar{\rho}V_{\rm min}$, which determines an $S_{\rm min}$. (Typically, this value is larger than that on which the walk first crossed below δ_v.) So we check if the walk remains below the barrier $B_{V_{\rm min}}(m)$ (of equation 2) for all $s(m) < S_{\rm min}$. If it does, we store this value and proceed to the next walk. If it does not, then we select the first of all steps larger than $S_{\rm min}$ which are below δ_v, and repeat the algorithm above until a void is identified, or until $S_{\rm min}$ becomes sufficiently large that the associated void size is negligibly small.

In the large mass (or volume) regime where the δ_v (no void-in-cloud) and δ_v–δ_c (Lagrangian void-in-cloud) distributions are similar, our algorithm predicts about a factor of 2 fewer voids. On smaller scales, where the δ_v–δ_c prediction is dropping sharply, ours predicts more voids – though it is still about a factor of 3 smaller than when the void-in-cloud problem has been ignored altogether. This quantifies the discussion at the end of the previous section about the expected differences between these three ways of estimating void abundances.

It turns out to be interesting to classify the voids identified by our new algorithm in terms of the number of times we had to loop

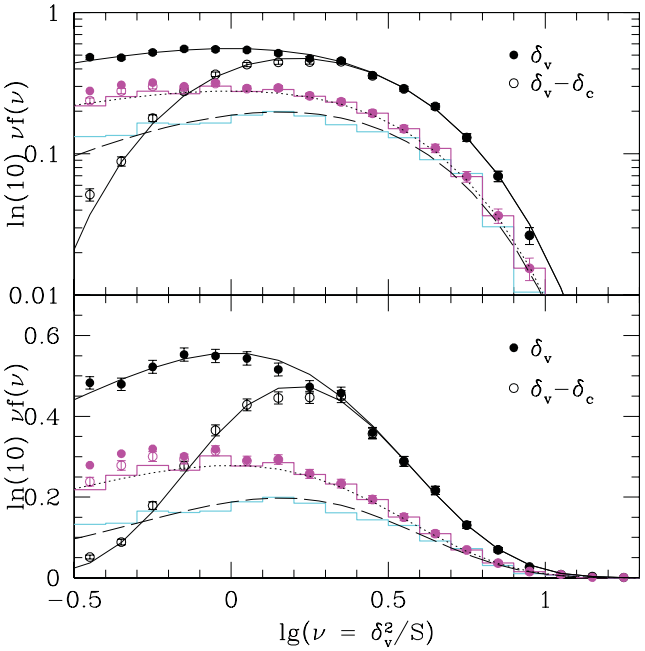

Figure 2. Monte Carlo solution of various excursion-set-based predictions for void abundances. Filled circles show the first crossing distribution of a single barrier of height δ_v; open circles show the distribution of the subset of walks which did not first cross δ_c; histograms show the distribution associated with our new algorithm. The black symbols and cyan histogram are for walks with uncorrelated steps, while the magenta symbols and histogram (which lie very close to each other) are for walks with correlated steps (see text for details). (For clarity, we only show error bars for the open circles in this case.) The differences between the symbols and the corresponding histograms are much more pronounced for walks with uncorrelated steps. Solid curves show the corresponding analytic solutions for walks with uncorrelated steps, for the single barrier and two-constant barrier cases. Dashed curve shows two times the distribution $Sf_0(S)$ derived in Appendix A (equation A13), and provides an excellent description of the cyan histogram. Dotted curve shows the expected solution for walks with completely correlated steps, which describes our results for correlated steps rather well.

through the algorithm. This is because, in Appendix A, we describe an analytic estimate of the fraction of walks $f_0(S)$ for which a void is identified after only a single pass through the algorithm. This estimate is in good agreement with the fraction of such walks in our Monte Carlo simulations (not shown). Curiously, multiplying this analytic estimate (equation A13) by a factor of 2 provides an excellent description of the full set of void walks. This is shown as the dashed line in Fig. 2. We have not found a simple derivation of why this should have been the case. Integrating $2f_0(S)$ numerically over all S gives 0.234 as the Lagrangian volume fraction; this is in excellent agreement with our Monte Carlos. (The corresponding Eulerian volume fraction is a factor of 5 larger, i.e. 1.17, as mentioned previously.)

The magenta symbols and histogram show the corresponding results for walks with correlated steps. In practice, we transformed each walk with uncorrelated steps into one with correlations by applying smoothing filters of different scales following Bond et al. (1991): we apply the filter $W(kR_L)$ to the same set of numbers g_i as above to get $\delta_j^{(\rm corr)} = \sum_i g_i W(k_i R_{Lj})$. Here R_L is the Lagrangian length-scale related to mass m by $m = (4\pi/3)\bar\rho R_L^3$. In this case, the correlation depends on the form of the filter and on the shape of the initial linear theory power spectrum $P(k)$, since one needs to know which values of k_j and R_{Lj} to associate with the jth step. Once a power spectrum and filter are specified, this can be done by inverting the relations $j\Delta s = (2\pi^2)^{-1}\int_0^{k_j} {\rm d}k\, k^2 P(k)$ and $j\Delta s = (2\pi^2)^{-1}\int_0^{\infty} {\rm d}k\, k^2 P(k) W^2(kR_{Lj})$. We used a Gaussian smoothing filter $W(kR) = {\rm e}^{-(kR)^2/2}$ and $P(k) \propto k^{-1.2}$. We then subjected each correlated walk to the same analysis as for the uncorrelated walks.

Notice that, in contrast to when the steps were uncorrelated, now the three ways of estimating void abundances all give almost the same answer. The sense of the differences which are beginning to appear at small masses is easily understood: ignoring the void-in-cloud problem altogether overestimates the abundances relative to the Lagrangian void-in-cloud treatment. This is only a small effect because a correlated walk which crosses δ_v is much less likely to have crossed δ_c than an uncorrelated walk. Stated differently: most walks which crossed δ_v did not go into the disallowed ($>\delta_c$) region anyway, so removing them makes little difference. In turn, the Lagrangian void-in-cloud analysis slightly overestimates the abundances relative to our Eulerian void-in-cloud algorithm, because it only eliminates the voids that got completely crushed, but does not alter the sizes of those that got squeezed a little. Therefore, it tends to overestimate the sizes of the voids, but this only becomes a significant effect for rather small voids.

By a curious coincidence, the first crossing distribution for walks with 'completely correlated' steps in the presence of a single constant barrier of height δ_v,

$$sf_v^{(\rm cc)}(s) = \frac{1}{2}\frac{|\delta_v|}{\sqrt{2\pi s}}\,{\rm e}^{-\delta_v^2/2s} \qquad (3)$$

(Paranjape et al. 2011), shown by the dotted curve, provides a rather good description of our predicted distribution. Recall that this prediction assumes the walks are perfectly smooth, so there is no void-in-cloud problem to begin with.

First crossing distributions for walks with correlated steps are relatively insensitive to shape of the underlying power spectrum or the smoothing filter (Bond et al. 1991; Paranjape et al. 2011). This is also true for the problem studied here: Fig. 3 shows the result of using $P(k)$ for a flat ΛCDM model with $(\sigma_8, \Omega_m) = (0.8, 0.27)$, and top-hat smoothing filters. Note that the void-in-cloud problem only becomes noticeable for small voids – but that it is more noticeable than it was for the Gaussian filtered walks (compare filled and open circles here and in previous figure). In addition, the solution is now noticeably different from that for 'completely correlated' steps. The sense of both these trends is easily understood from the fact that Gaussian smoothing is known to produce smoother walks than top hat (Paranjape et al. 2011), so the results here are intermediate between those for sharp k and Gaussian smoothing.

4 DISCUSSION

We have presented what we believe to be a better excursion set treatment of the void-in-cloud problem (Section 2 and Fig. 1). In addition to accounting for the fact that some voids can be crushed completely if they are surrounded by an overdensity which collapses around them, our Eulerian-space-based approach also accounts for those voids which are squeezed rather than completely crushed. We argued that voids which are being squeezed by their surroundings may be the easiest to recognize observationally, so our modification is potentially an important one. In particular, our approach shows explicitly why, in some cases, a purely local Lagrangian-based prediction for the evolution yields the wrong answer; it can be thought of as an explicit demonstration of how stochasticity in the

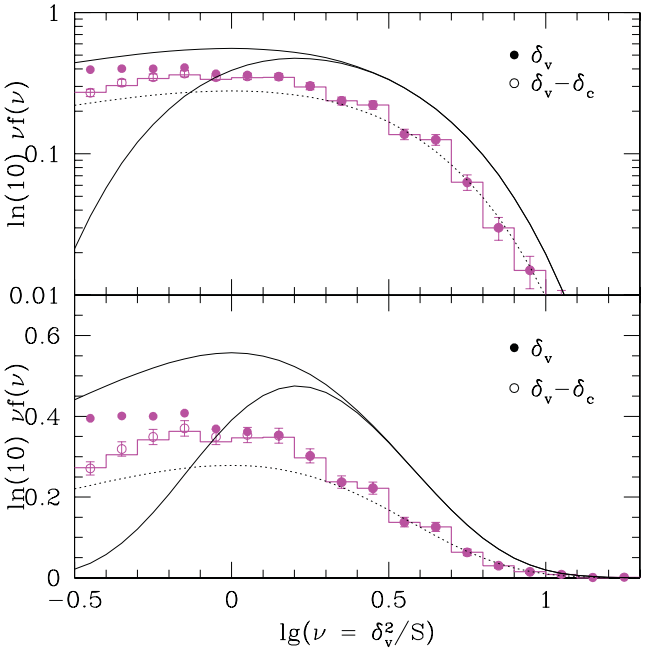

Figure 3. Monte Carlo distributions for walks with correlated steps with the same format as in Fig. 2, except that now Monte Carlos used a ΛCDM $P(k)$ and top-hat smoothing filters. The solid and dotted curves are the same as in Fig. 2.

mapping between the Lagrangian and Eulerian density fields can arise naturally.

The excursion set statement of the problem involves random walks. We provided an analytic expression (Appendix A) for the predicted distribution of void sizes for the case in which the walks have uncorrelated steps, and showed that it was in good agreement with numerical Monte Carlo solutions of the problem. (This expression suffers from a curious 'factor-of-two' problem which we discuss briefly – but we leave an exact solution of it to future work.) This analysis suggests that the void-in-cloud process modifies the predicted void size distribution significantly, so that our new treatment of it was necessary.

However, this conclusion depends strongly on whether or not we account for the correlations between scales in the initial density fluctuation field. In contrast to what happens for uncorrelated steps, for correlated steps, we found that the change in void abundances due to this effect is negligible for voids that are larger than V_*, where V_* is the characteristic Eulerian scale associated with voids: $V_* = 5M_*/\bar{\rho}$, where $\sigma(M_*) = |\delta_v|$. For flat ΛCDM with $(\Omega_m, \sigma_8) = (0.27, 0.8)$, this scale is $V_* \simeq (1.4\,h^{-1}\,\mathrm{Mpc})^3$ at $z \sim 0$; larger voids have not been squeezed by their surroundings. Since voids identified in most galaxy catalogues are typically much larger, it may be unnecessary to account for the void-in-cloud process when interpreting observations. In this case, the void size distribution is quite well approximated by that of a single barrier, for which good analytic approximations are available (Paranjape et al. 2011).

Although our results provide increased understanding of void abundances and evolution, a number of issues must be addressed before they can be used to provide useful constraints on cosmology. First, the correlated walk problem is known to underpredict the abundances of clusters (Bond et al. 1991). Paranjape et al. (2011) describe at least three possible resolutions, which have to do with the fundamental assumptions which the excursion set approach uses to relate the first crossing distribution with halo abundances. Presumably, this problem, and hence the potential resolutions, also apply to voids. Secondly, we must include a model for transforming our knowledge of voids in the dark matter distribution to underdensities in the galaxy distribution. This will require applying the analysis of Furlanetto & Piran (2006) to our new formula for void abundances, perhaps accounting for the fact that the voids have non-trivial internal density profiles (Patiri et al. 2006a, following Sheth 1998).

ACKNOWLEDGMENTS

We thank the anonymous referee for helpful comments which significantly improved the manuscript. TYL was supported by the World Premier International Research Center Initiative (WPI Initiative), MEXT, Japan and a JSPS travel grant (Institutional Program for Young Researcher Overseas Visits). He is grateful to the Center for Particle Cosmology at the University of Pennsylvania and to ICTP for their hospitality in 2010 and 2011, respectively. RKS is supported in part by NSF-AST 0908241.

REFERENCES

Bernardeau F., 1994, ApJ, 427, 51
Biswas R., Alizadeh E., Wandelt B. D., 2010, Phys. Rev. D, 82, 023002
Blumenthal G. R., da Costa L. N., Goldwirth D. S., Lecar M., Piran T., 1992, ApJ, 388, 234
Bond J. R., Cole S., Efstathiou G., Kaiser N., 1991, ApJ, 379, 440
D'Amico G., Musso M., Noreña J., Paranjape A., 2011, Phys. Rev. D, 83, 023521
Dubinski J., da Costa L. N., Goldwirth D. S., Lecar M., Piran T., 1993, ApJ, 410, 458
Epstein R. I., 1983, MNRAS, 205, 207
Furlanetto S. R., Piran T., 2006, MNRAS, 366, 467
Gradshteyn I. S., Rhyzik I. M., 2007, Tables of Integrals, Series and Products, 7th edn. Elsevier, Amsterdam
Gunn J. E., Gott J. R., III, 1972, ApJ, 176, 1
Hoyle F., Vogeley M., 2004, ApJ, 607, 751
Hoyle F., Rojas R. R., Vogeley M. S., Brinkmann J., 2005, ApJ, 620, 618
Kamionkowski M., Verde L., Jimenez R., 2009, J. Cosmol. Astropart. Phys., 01, 010
Kauffmann G., Fairall A. P., 1991, MNRAS, 248, 313
Lacey C., Cole S., 1993, MNRAS, 262, 627
Lam T. Y., Sheth R. K., 2008, MNRAS, 386, 407
Lam T. Y., Sheth R. K., Desjacques V., 2009, MNRAS, 399, 1482
Lavaux G., Wandelt B. D., 2010, MNRAS, 403, 1392
Maggiore M., Riotto A., 2010, ApJ, 711, 907
Martino M., Sheth R. K., 2009, Phys. Rev. D, submitted (arXiv:0911.1829)
Martino M., Stabenau H. F., Sheth R. K., 2009, Phys. Rev. D, 79, 084013
Pan D., Vogeley M. S., Hoyle F., Choi Y.-Y., Park C., 2011, preprint (arXiv:1103.4156)
Paranjape A., Lam T. Y., Sheth R. K., 2011, MNRAS, in press (doi:10.1111/j.1365-2966.2011.20128.x (arXiv:1105.1990)
Park D., Lee J., 2007, Phys. Rev. Lett., 98, 081301
Patiri S. G., Betancort-Rijo J. E., Prada F., 2006a, MNRAS, 368, 1132
Patiri S. G., Betancort-Rijo J. E., Prada F., Klypin A., Gottlöber S., 2006b, MNRAS, 369, 335
Peacock J. A., Heavens A. F., 1990, MNRAS, 243, 133
Press W. H., Schechter P., 1974, ApJ, 187, 425
Sheth R. K., 1998, MNRAS, 300, 1057
Sheth R. K., van de Weygaert R., 2004, MNRAS, 350, 517
Sheth R. K., Mo H. J., Tormen G., 2001, MNRAS, 323, 1
van de Weygaert R., van Kampen E., 1993, MNRAS, 263, 481

APPENDIX A: THE FIRST CROSSING DISTRIBUTION FOR WALKS WITH UNCORRELATED STEPS

In this appendix we sketch the derivation of the first crossing distribution $f_0(S)$ (for walks with uncorrelated steps) discussed in Section 3, which counts the fraction of walks that survive one pass through our algorithm. The analysis is tractable when the void-in-cloud barriers are linear, which happens for a power spectrum $P(k) \propto k^{-1.2}$. It is then convenient to think of the barrier $B_V(m)$ as a function of $s = s(m)$, parametrized by the value $S = s(M = 0.2\bar{\rho}V)$ at which the barrier crosses the constant barrier δ_v. We use the notation $B_S(s)$ to denote the void-in-cloud barrier, and equation (2) translates to $B_S(s) = \delta_c - (\delta_T/S)s$, where $\delta_T \equiv \delta_c + |\delta_v|$.

We are after the fraction of walks which satisfy the following conditions.

(i) They first cross the barrier $B_S(s)$ at $s = S' < S$, without having crossed δ_v before S'.

(ii) They first cross the barrier $B_{S+\Delta S}(s)$ *after* this barrier has passed through δ_v, i.e. at $s > S + \Delta S$.

We evaluate the resulting fraction in the limit $\Delta S \to 0$, and interpret it as $\Delta S f_0(S)$.

The first condition above requires us to compute the fraction of walks $\mathrm{d}S'\mathcal{F}_B(S')$ which first cross $B_S(s)$ in the interval $s \in (S', S' + \mathrm{d}S')$, without having crossed δ_v before. The second condition requires the fraction $\mathrm{d}s f_{B\Delta}(s|S', B_S(S'))$ of walks that started at height $B_S(S')$ on scale S' and then went on to first cross $B_{S+\Delta S}(s)$ in the range $(s, s + \mathrm{d}s)$. The distribution $f_0(S)$ is then given by

$$\Delta S f_0(S) = \int_0^S \mathrm{d}S' \mathcal{F}_B(S') \int_{S+\Delta S}^{\infty} \mathrm{d}s\, f_{B\Delta}(s|S', B_S(S')). \tag{A1}$$

The distribution $\mathcal{F}_B(s)$ can be written in a form which allows a recursive calculation: we first count the fraction of walks $f_B(s)$ which first cross B_S at $s < S$, regardless of whether they crossed δ_v, and then subtract those which did cross δ_v prior to s. We then have

$$\mathcal{F}_B(s) = f_B(s) - \int_0^s \mathrm{d}s'\, \mathcal{F}_v(s')\, f_B(s|s', \delta_v), \tag{A2}$$

where $\mathcal{F}_v(s')$ (with $s' < S$) denotes the distribution of first crossing of δ_v without crossing B_S, and the integral in the second term is counting walks that reached δ_v at s' for the first time without crossing B_S, and then reached B_S for the first time at s. A similar argument, with the roles of B_S and δ_v interchanged, allows us to write

$$\mathcal{F}_v(s') = f_v(s') - \int_0^{s'} \mathrm{d}s''\, \mathcal{F}_B(s'')\, f_v(s'|B_S, s''), \tag{A3}$$

where $f_v(s')$ is the distribution of first crossing of δ_v whether or not it had first crossed B_S, and $f_v(s'|B_S, s'')$ is the corresponding conditional distribution. Notice that, despite the compact notation, both the distributions $\mathcal{F}_B(s)$ and $\mathcal{F}_v(s)$ depend on the scale S which parametrizes the barrier $B_S(s)$. Repeated substitution of $\mathcal{F}_B(s)$ in the expression for $\mathcal{F}_v(s)$, and vice versa, gives rise to an alternating series, the successive terms of which describe walks which cross δ_v after more and more zigzags.

As an aside, we note that when $B_S(s) = \delta_c$ for all s, independent of S (i.e. the Sheth–van de Weygaert model in which δ_c is parallel to δ_v), then the integrals in the expressions above can be done analytically, yielding

$$\mathcal{F}_v(s) = \mathcal{F}_{\mathrm{SvdW}}(s, \delta_v, \delta_c) \equiv f_v(s) - f_{c+T}(s) + f_{v+2T}(s) - \cdots, \tag{A4}$$

where c, v and T in the expression above denote δ_c, $|\delta_v|$ and $\delta_T = \delta_c + |\delta_v|$ (Lam et al. 2009; D'Amico et al. 2011). The distribution $\mathcal{F}_B$ in this case is given simply by interchanging the roles of δ_c and δ_v in $\mathcal{F}_v$. In this case, the first few terms dominate – walks with many zigzags from one barrier to the other are rare – so truncating the series yields a good approximation to the full answer. In particular, when $\delta_T \gg |\delta_v|$ then the first term dominates for small S: for the largest voids, the void-in-cloud problem is irrelevant.

However, when $B_S(s)$ is a decreasing function of s, which eventually crosses δ_v, then truncating the series is dangerous, because close to the point where the two barriers cross, zigzags are no longer large, so many can occur. The first crossing distribution then becomes very sensitive to the exact relation between the first crossing scale, and the scale at which the barriers cross. We are interested in the case when $B_S(s) = \delta_c - (\delta_T/S)s$ is a linear barrier. The expression for $\mathcal{F}_v$ above can then be solved exactly. Since the full proof involves some rather tedious integrals, we only present a sketch here highlighting the main ingredients. Equations (A2) and (A3) can be combined as

$$\mathcal{F}_v(s') = f_v(s') + \mathcal{I}_1 + \mathcal{I}_2, \tag{A5}$$

where

$$\begin{aligned}
\mathcal{I}_1(s') &= -\int_0^{s'} \mathrm{d}s\, f_v(s'|s, B_S(s))\, f_B(s), \\
\mathcal{I}_2(s') &= \int_0^{s'} \mathrm{d}s_1\, f_v(s'|s_1, B_S(s_1)) \\
&\quad \times \int_0^{s_1} \mathrm{d}s_2\, f_B(s_1|s_2, \delta_v)\mathcal{F}_v(s_2).
\end{aligned} \tag{A6}$$

The conditional distributions simplify as in the two-constant barrier case, due to the Markovian nature of the walks. Unlike this previous case, however, this time the single barrier distributions f_v and f_B are fundamentally different from each other. Whereas f_v is the same as before for a single constant barrier, $f_v(s) = (2\pi s^3)^{-1/2}|\delta_v|\mathrm{e}^{-\delta_v^2/2s}$, f_B for a single linear barrier $B_S(s)$ is now given by the inverse Gaussian (Sheth 1998),

$$f_B(s) = f_{\mathrm{IG}}(s, B_S(s)) \equiv \frac{B_S(0)}{(2\pi s^3)^{1/2}}\, \mathrm{e}^{-B_S(s)^2/2s}. \tag{A7}$$

Since the distribution $\mathcal{F}_v(s)$ appears in the integral in $\mathcal{I}_2$, the basic strategy is to recursively use equation (A5) and solve for $\mathcal{F}_v(s)$. For example, the integral in $\mathcal{I}_1$ above reduces to

$$\mathcal{I}_1(s) = -\frac{(2\delta_c + |\delta_v|)}{\sqrt{2\pi s^3}} \mathrm{e}^{-\delta_v^2/2S} \mathrm{e}^{-(1/2s)(2\delta_c+|\delta_v|)^2(1-s/S)}. \tag{A8}$$

In practice we compute the first few terms of the recursive series, which clearly reveal a pattern that closely mimics the one in equation (A4), but with a rescaled argument for the single barrier distributions. We are left with

$$\mathcal{F}_v(s) = \left(1 - \frac{s}{S}\right)^{-3/2} \mathrm{e}^{-\delta_v^2/2S} \mathcal{F}_{\mathrm{SvdW}}\left(\frac{s}{1 - s/S}, \delta_v, \delta_c\right), \tag{A9}$$

where $\mathcal{F}_{\mathrm{SvdW}}(t, \delta_v, \delta_c)$ was defined in equation (A4). For the interested reader, the integrals appearing in the derivation of

equation (A9) involve repeated use of the identities (for $A, B > 0$):

$$\int_0^1 \frac{\mathrm{d}y}{y^{3/2}} \frac{1}{(1-y)^{3/2}} \, \mathrm{e}^{-(A^2/2y)-[B^2/2(1-y)]} = \sqrt{2\pi} \frac{A+B}{AB} \, \mathrm{e}^{-(1/2)(A+B)^2},$$
$$\int_0^1 \frac{\mathrm{d}y}{y^{1/2}} \frac{1}{(1-y)^{3/2}} \, \mathrm{e}^{-(A^2/2y)-[B^2/2(1-y)]} = \frac{\sqrt{2\pi}}{B} \, \mathrm{e}^{-(1/2)(A+B)^2}, \tag{A10}$$

which can be proved using the relation 3.472(5) of Gradshteyn & Rhyzik (2007).

Using equation (A9) in equation (A2) leads to an expression for $\mathcal{F}_B(S')$, which can then be used in equation (A1) to obtain an expression for $f_0(S)$, after substituting for the conditional distribution $f_{B\Delta}(s|S', B_S(S'))$ using

$$f_{B\Delta}(s|S', B_S(S')) = f_{\rm IG}(s - S', B_{S+\Delta S}(s) - B_S(S')), \tag{A11}$$

which follows from the Markovianity of the walks, with $f_{\rm IG}$ defined in equation (A7). Notice that, in the limit $\Delta S \to 0$, the evaluation of $B_{S+\Delta S}(s) - B_S(S')$ at $s = S'$ becomes proportional to ΔS, and hence the remaining expression for $f_0(S)$ can be evaluated at $\Delta S = 0$. Unfortunately, not all of the resulting integrals can be performed analytically. It turns out to be better to use the series for $\mathcal{F}_{\rm SvdW}$ given in equation (1) of Sheth & van de Weygaert (2004),

$$\mathcal{F}_{\rm SvdW}(t, \delta_{\rm v}, \delta_{\rm c}) = \sum_{j=1}^{\infty} \frac{j\pi}{\delta_{\rm T}^2} \sin\left(\frac{j\pi|\delta_{\rm v}|}{\delta_{\rm T}}\right) \mathrm{e}^{-(j^2\pi^2/2\delta_{\rm T}^2)t}, \tag{A12}$$

which is equivalent to the one in equation (A4) (D'Amico et al. 2011). This allows us to bring the expression for f_0 to the following form:

$$Sf_0(S) = \frac{1}{\sqrt{2\pi}} \mathrm{e}^{-\nu_{\rm v}^2/2} \, [\mathcal{A} - \mathcal{B}], \tag{A13}$$

where

$$\mathcal{A} = \nu_{\rm c}\nu_{\rm T} \, \mathrm{e}^{\nu_{\rm c}^2/2} \left(\sqrt{2\pi} \, \mathrm{erfc}\left(\frac{\nu_{\rm c}}{\sqrt{2}}\right) - \nu_{\rm T} \, \mathrm{e}^{\nu_{\rm T}^2/2} \, \mathrm{I}(\nu_{\rm c}, \nu_{\rm T})\right), \tag{A14}$$

$$\mathcal{B} = \sum_{j=1}^{\infty} j\pi \sin\left(\frac{j\pi|\delta_{\rm v}|}{\delta_{\rm T}}\right) \left[\frac{4\nu_{\rm T}}{j^2\pi^2} - \frac{2}{\nu_{\rm T}} \, \mathrm{e}^{j^2\pi^2/2\nu_{\rm T}^2} \Gamma\left(0, \frac{j^2\pi^2}{2\nu_{\rm T}^2}\right) + \sqrt{2\pi} \, \mathrm{II}(j, \nu_{\rm T}) - \nu_{\rm T} \, \mathrm{III}(j, \nu_{\rm T})\right], \tag{A15}$$

and we used the notation $\{\nu_{\rm v}, \nu_{\rm c}, \nu_{\rm T}\} \equiv \{|\delta_{\rm v}|, \delta_{\rm c}, \delta_{\rm T}\}/\sqrt{S}$ and defined the integrals

$$\mathrm{I}(\nu_{\rm c}, \nu_{\rm T}) = \int_0^1 \frac{\mathrm{d}y}{\sqrt{y}} \exp\left(-\frac{\nu_{\rm T}^2 y}{2} - \frac{\nu_{\rm c}^2}{2y}\right) \times \mathrm{erfc}\left(\frac{\nu_{\rm T}}{\sqrt{2}}\sqrt{1-y}\right), \tag{A16}$$

$$\mathrm{II}(\mathrm{j}, \nu_{\rm T}) = \int_0^1 \frac{\mathrm{d}y}{\sqrt{y}} \exp\left(-\frac{\nu_{\rm T}^2 y}{2} - \frac{j^2\pi^2(1-y)}{2\nu_{\rm T}^2 y}\right) \times \mathrm{erfc}\left(\frac{\nu_{\rm T}\sqrt{y}}{\sqrt{2}}\right), \tag{A17}$$

$$\mathrm{III}(\mathrm{j}, \nu_{\rm T}) = \int_0^1 \frac{\mathrm{d}x}{x} \exp\left(-\frac{j^2\pi^2(1-x)}{2\nu_{\rm T}^2 x}\right) \times \int_0^1 \frac{\mathrm{d}y}{(1-y)^{3/2}} (1 - xy) \exp\left(-\frac{\nu_{\rm T}^2 x}{2} \frac{y^2}{1-y}\right) \times \mathrm{erfc}\left(\frac{\nu_{\rm T}\sqrt{xy}}{\sqrt{2}}\right), \tag{A18}$$

which must be performed numerically. We have checked that the result (after keeping ∼600 terms in the sum over j) accurately describes the fraction of walks which survive one pass through our numerical algorithm, as it should.

As noted in the text, we find that two times $f_0(S)$ provides an excellent description for the full Monte Carlo distribution obtained by our algorithm. This is shown as the dashed line in Fig. 2. In fact, if we write this factor of 2 as follows:

$$Sf(S) = 2\,Sf_0(S) = \frac{Sf_0(S)}{1 - 1/2} = Sf_0(S) \sum_{n=0}^{\infty} 2^{-n}, \tag{A19}$$

then the nth term in the sum above approximates the distribution associated with the set of walks which required $n + 1$ loops through our algorithm. While this is highly suggestive of a resummation of 'loops', with the 'tree-level' result being $f_0(S)$, we have not found a simple demonstration of why this should be the case.

This paper has been typeset from a TEX/LATEX file prepared by the author.